



Published in final edited form as:

*Signal Transduct Target Ther.* 2016 ; 1: . doi:10.1038/sigtrans.2016.30.

## Tumor cell-intrinsic PD-L1 promotes tumor-initiating cell generation and functions in melanoma and ovarian cancer

Harshita B. Gupta<sup>1</sup>, Curtis A. Clark<sup>2</sup>, Bin Yuan<sup>3</sup>, Gangadhara Sareddy<sup>4</sup>, Srilakshmi Pandeswara<sup>1</sup>, Alvaro S. Padron<sup>1</sup>, Vincent Hurez<sup>1</sup>, José Conejo-Garcia<sup>5</sup>, Ratna Vadlamudi<sup>1,2,4,6</sup>, Rong Li<sup>2,3,6</sup>, and Tyler J. Curiel<sup>1,2,6,7,\*</sup>

<sup>1</sup>Department of Medicine, University of Texas Health Science Center, San Antonio, TX 78229

<sup>2</sup>The Graduate School of Biomedical Sciences, University of Texas Health Science Center, San Antonio, TX 78229

<sup>3</sup>Department of Molecular Medicine, University of Texas Health Science Center, San Antonio, TX 78229

<sup>4</sup>Department of Obstetrics and Gynecology, University of Texas Health Science Center, San Antonio, TX 78229

<sup>5</sup>Tumor Microenvironment and Metastasis Program, The Wistar Institute, Philadelphia, PA 19104

<sup>6</sup>Cancer Therapy & Research Center, University of Texas Health Science Center, San Antonio, TX 78229

<sup>7</sup>Department of Microbiology and Immunology, University of Texas Health Science Center, San Antonio, TX 78229

### Abstract

As tumor PD-L1 provides signals to anti-tumor PD-1<sup>+</sup> T cells that blunt their functions, αPD-1 and αPD-L1 antibodies have been developed as anti-cancer immunotherapies based on interrupting this signaling axis. However, tumor cell-intrinsic PD-L1 signals also regulate immune-independent tumor cell proliferation and mTOR signals, among other important effects. Tumor initiating cells (TIC) generate carcinomas, resist treatments and promote relapse. We show here that in murine B16 melanoma and ID8agg ovarian carcinoma cells, TIC express more PD-L1 versus non-TIC. Silencing PD-L1 in B16 and ID8agg cells by shRNA (“PD-L1<sup>lo</sup>”) reduced TIC numbers, the canonical TIC genes *nanog* and *pou5f1* (*oct4*), and functions as assessed by tumorsphere development, immune-dependent and immune-independent tumorigenesis, and serial transplantability *in vivo*. Strikingly, tumor PD-L1 sensitized TIC to interferon-γ and rapamycin *in vitro*. Cell-intrinsic PD-L1 similarly drove functional TIC generation, canonical TIC gene expression, and sensitivity to interferon-γ and rapamycin in human ES2 ovarian cancer cells. Thus, tumor-intrinsic PD-L1 signals promote TIC generation and virulence, possibly by promoting

\*To whom correspondence should be addressed: Tyler Curiel, MD, MPH, Department of Medicine, University of Texas Health Science Center at San Antonio, STRF MC 8252, 8403 Floyd Curl Drive, San Antonio, TX 78229-3900, USA. Phone: 210-562-4083, curielt@uthscsa.edu.

The authors disclose no potential conflicts of interest

canonical TIC gene expression, suggesting that PD-L1 has novel signaling effects on cancer pathogenesis and treatment responses.

## Keywords

B7-H1; PD-L1; PD-1; mTOR; tumor initiating cell; melanoma; ovarian cancer; human

## Introduction

PD-L1 (CD274, B7-H1) is an immune co-signaling molecule in the B7-H (B7 homology) family. It plays a key role in maintaining an immunosuppressive tumor environment by negatively regulating anti-tumor responses through fostering apoptosis, anergy or exhaustion of PD-1 expressing T cells, and is thus immunopathogenic in many cancers (1, 2). Immune checkpoint blockade with anti-PD-L1 monoclonal antibodies ( $\alpha$ PD-L1) is clinically effective in many cancer models. The  $\alpha$ PD-L1 antibody atezolizumab was recently FDA approved to treat certain bladder and lung cancers. Its principal mode of action is thought to be protecting anti-tumor T cells from inhibition by tumor surface-expressed PD-L1 (1, 2). We recently reported that PD-L1 also mediates important cell-intrinsic signals that regulate immune-independent tumor growth, mTOR signaling and autophagy in melanoma and ovarian cancer cells (3). Tumor-intrinsic PD-L1 also regulates tumor glucose metabolism regulation, affecting anti-tumor T cells (4). Thus, cell-intrinsic PD-L1 signals merit further studies.

Tumors are comprised of genetically and functionally heterogeneous cell populations. Among these are tumor initiating cells (TIC), initially reported in hematologic cancers, but that also give rise to epithelial carcinomas (5, 6). Despite their importance, mechanisms for TIC generation and virulence are incompletely understood.

Because TIC are resistant to many therapies, and can give rise to tumor relapse, much attention has been given to targeting them for treatment (5, 6). PD-L1 and PD-1 are expressed on TIC (7–10) but definitive evidence for their roles in TIC generation have not been reported to our knowledge. We demonstrate here that tumor cell-intrinsic PD-L1 directly drives the generation and functions of TIC in murine melanoma and ovarian cancer cells, and a human ovarian cancer cell line. Tumor PD-L1 is well-known to give negative cell-extrinsic signals to PD-1<sup>+</sup> T cells, but we now show that tumor PD-L1 also appears to generate intra-tumor cell signals that augment canonical TIC gene expression, regulate TIC numbers and functions, and sensitize them to rapamycin and interferon- $\gamma$ . These previously unknown intracellular signaling effects define important new mechanisms for PD-L1 participation in cancer immunopathogenesis and suggests novel treatment strategies.

## Materials and Methods

### Mice

Male and female wild type (WT) C57BL/6J (BL6) and NOD.Cg-Prkdc<sup>scid</sup>Il2rg<sup>tm1Wj1</sup>/SzJ [non-obese diabetic/severe combined immunodeficiency (NOD/SCID)/interleukin (IL)-2R $\gamma$  KO, NSG] mice were purchased from Jackson Laboratory, maintained under specific

pathogen free conditions and given food and water *ad libitum*. 8 to 10-week old age- and sex-matched mice were used for experiments. All animal studies were approved by our Institutional Animal Care and Use Committee.

### Cell lines and transfections

The murine ovarian cancer cell line ID8, a gift from George Coukos, University of Pennsylvania, is a well-accepted transplantable mouse model that produces tumors replicating important aspects of human ovarian cancer, including local spread and ascites after intraperitoneal (i.p.) injection into syngeneic BL6 mice (11). We generated an aggressive ID8 line (ID8agg) by serial passage through WT mice (3). The murine melanoma B16-F10 cell line (herein “B16”) and the human ovarian cancer cell line ES2 were purchased from the American Type Culture Collection. Cells were not re-authenticated for this work. Mouse cells are on the BL6 background. Cells were used in passages <5 and maintained in 5% fetal bovine serum-containing medium RPMI-1640 plus 1% penicillin/streptomycin, 1% L-glutamate, and 1% HEPES buffer (complete medium). B16, ID8agg and human ES2 cells with stable PD-L1 knock down were generated and described in our recent report (3). Briefly, cells were transfected with murine or human control shRNA (“control”) or shRNA against PD-L1 (“PD-L1<sup>lo</sup>”). Monoclonal cells were selected in puromycin and PD-L1 expression status confirmed by flow cytometry and Western blotting.

### In vitro conditions and treatments

All cells were cultured under identical conditions, including cell density and passage number, and studied at ~80% confluency on 100 mm plastic culture plates in complete medium. Indicated cultures included rapamycin (Sigma) or mouse recombinant interferon- $\gamma$  (R&D Systems) for 48 hours (B16 and ID8agg) or 60 hours (ES2) at concentrations shown. Cell viability and numbers were determined on a Vi-Cell XR (Beckman Coulter) or hemocytometer and stained as described below. Dimethylsulphoxide (DMSO) (Sigma) or PBS were used as negative controls (vehicle) for rapamycin or interferon- $\gamma$ , respectively.

### Flow cytometry

Cells were stained and sorted as previously described (12), using BD LSRII and FACSAriaII hardware and analyzed by FACSDiva (BD Bioscience) or FlowJo (FlowJo LLC) software. Zombie Yellow Fixable Viability kit, anti-mouse PD-L1 (B<sub>v</sub>421, clone 10F.9G2), CD44 (PerCP-Cy5), CD133 (PE-Cy7), CD24 (PE), anti-human CD44 (Per-CP-Cy5), CD24 (PE), PD-L1 (PE-Cy7, clone 29E.2AE) and matched isotype controls were purchased from BioLegend. ALDEFLUOR kits were purchased from STEMCELL technologies. The ALDEFLUOR assay was done with  $1 \times 10^6$  ES2 cells/ml. 5  $\mu$ L of the specific aldehyde dehydrogenase (ALDH) inhibitor diethylaminobenzaldehyde was added to control tubes. Tubes were incubated with 5  $\mu$ L BODIPY-aminoacetaldehyde, a fluorescent substrate for ALDH and incubated for 45 min at 37° C. Following washes, samples were kept at 4° C for remaining staining. TIC were defined as CD44<sup>+</sup>CD133<sup>+</sup>CD24<sup>+</sup> [B16 (13)], CD44<sup>+</sup>CD24<sup>+</sup> [ID8 (14)], and ALDH<sup>hi</sup> or CD44<sup>+</sup>CD24<sup>-</sup> (as indicated, ES2) (15, 16) by flow cytometry.

### ***In vivo* cell challenges, treatments and assessments**

WT or NSG mice were injected with indicated numbers of B16 cells or corresponding TIC subcutaneously (s.c.) (17), or ID8agg cells or corresponding TIC i.p. B16 growth was measured with Vernier calipers and tumor volume calculated as  $(\text{length} \times \text{width}^2)/2$ . Survival was determined by tumor size  $\geq 1800 \text{ mm}^3$  or animal distress. ID8agg survival was determined by ascites formation or distress (18). For serial re-transplantation, tumors were removed under sterile conditions when they reached  $1800 \text{ mm}^3$ , digested, stained for viability and  $10^4$  sorted TICs were injected into naive NSG mice s.c. For ES2 TIC, female NSG mice were challenged with 20,000 sorted ALDH<sup>hi</sup> TIC i.p. The survival of these mice was determined by ascites accumulation causing weight  $\geq 130\%$  of baseline, or distress.

### **Tumorsphere formation**

$10^4$  TICs were sorted from cultures and grown in DMEM-F12 medium (Gibco) with B27 (Invitrogen), 20 ng/ml epidermal growth factor (PeproTech) and 20 ng/ml fibroblast growth factor (PeproTech) (14) for one-two weeks in  $25 \text{ cm}^2$  flasks. At least 6 fields/clone were counted. Spheroid images were taken and analyzed using QCapture Pro 6.0 software. Diameter was calculated using the  $100 \mu\text{m}$  measurement bar.

### **Quantitative RT-PCR**

Total RNA was isolated from cells using a Direct-zol RNA miniprep kit (Zymo Research). cDNA was synthesized with  $1 \mu\text{g}$  total RNA using the ImPromII Reverse Transcription System (Promega) and random primers. Quantitative PCR (qPCR) was conducted using the 7900HT Real-Time PCR System (Applied Biosystems), amplified with Taqman gene expression assays (Applied Biosystems) for mouse *nanog* (Mm02019550\_s1), *sox2* (Mm03053810\_s1), *pou5f1* (*oct4*, Mm03053917\_g1) and *rptor* (Mm01242613\_m1) according to the manufacturer's instructions with  *$\beta$ -actin* (Mm02619580\_g1) as the internal control. ES2 *NANOG* (Hs04399610\_g1), *OCT4* (Hs00999632\_g1), *SOX2* (Hs01053049\_s1), *RPTOR* (Hs00375332\_m1) and *GAPDH* were amplified in like fashion. Fold changes were calculated by  $2^{-\Delta\Delta\text{CT}}$  between TIC and respective total cultures and P value calculated by unpaired *t* test. These fold changes were compared between control and PD-L1<sup>lo</sup> cells by unpaired *t* test.

### **Statistical analysis**

Statistical analyses were conducted using Prism software (GraphPad). Data were plotted as means  $\pm$  SEM. For tumor growth, two-way ANOVA plus Bonferroni post-tests was used to compare replicate means. Unpaired *t* test was used for comparison between individual means. Kaplan-Meier estimates and the log-rank test were used to analyze survival.  $P < 0.05$  was considered significant.

## **Results**

### **TIC express higher PD-L1 and PD-1 versus non-TIC**

We investigated TIC PD-L1 expression on B16 and ID8agg cells by flow cytometry using well-accepted markers for each cell line (13, 14)(and see **Methods** and Suppl. Fig. 1–2).

Both tumor lines expressed PD-L1, but interestingly, PD-L1 expression on B16 (Fig. 1A) and ID8agg (Fig. 1B) TIC was higher than respective non-TIC. Differential PD-L1 on TIC versus non-TIC was more pronounced in B16 (PD-L1 mean fluorescence intensity [MFI] of control B16 TIC versus non-TIC 4860 versus 1590, for PD-L1<sup>lo</sup> clone 4 1223 versus 589 and clone 10 2075 versus 941); for control ID8agg TIC versus non-TIC 261 versus 215, PD-L1<sup>lo</sup> clone 3 132 versus 93 and clone 6 209 versus 161 for TIC versus non-TIC, respectively). B16 and ID8agg PD-L1<sup>lo</sup> TIC expressed lower PD-L1 versus their respective control TIC (Fig. 1A, B) further validating the PD-L1 knock down. B16 TIC express significant PD-1 consistent with a recent report (19), whereas B16 non-TIC expressed negligible PD-1. Similarly, ID8agg TIC expressed PD-1 whereas ID8agg non-TIC PD-1 expression was negligible. In both cell lines, PD-1 expression was similar in control versus PD-L1<sup>lo</sup> TIC independent of PD-L1 expression (Fig. 1C, D).

### Tumor PD-L1 regulates TIC numbers

We recently reported RNA-seq data from ID8agg cells suggesting that cell-intrinsic PD-L1 controls canonical signaling pathways governing cell differentiation including mTOR. We also showed that PD-L1<sup>lo</sup> B16 and ID8agg tumors grow slower versus respective control cells in immune deficient mice (3). Thus, we hypothesized that PD-L1 signals could contribute to TIC generation as a mechanism for reduced growth kinetics and tumorigenicity. *In vitro* cultures of PD-L1<sup>lo</sup> B16 cells had significantly fewer CD44<sup>+</sup>CD133<sup>+</sup>CD24<sup>+</sup> TIC versus control B16 cultures (Fig. 1E), and PD-L1<sup>lo</sup> ID8agg cell cultures had significantly fewer CD44<sup>+</sup>CD24<sup>+</sup> TIC versus PD-L1<sup>lo</sup> ID8agg cell cultures (Fig. 1F). Thus, tumor PD-L1 is a candidate regulator of TIC generation in melanoma and ovarian cancer cells.

### PD-L1 promotes TIC tumorosphere formation *in vitro*

A key functional aspect of TIC is self-renewal, studied *in vitro* as tumorosphere formation (20). PD-L1<sup>lo</sup> TIC from B16 and ID8agg exhibited significantly reduced numbers and size of tumorospheres versus respective control TIC (Fig. 2A, B), consistent with defective PD-L1<sup>lo</sup> TIC self-renewal function *in vitro*.

### PD-L1 promotes immune-independent TIC growth and virulence *in vivo*

For *in vivo* functional assessment, control B16 TIC were challenged into WT mice, producing tumors with significantly shorter latency versus PD-L1<sup>lo</sup> TIC (median 70 days versus >180 days [never reached, experiment terminated], respectively, Fig. 2C). In fact, no mouse challenged with PD-L1<sup>lo</sup> TICs formed tumors. Confirming tumorigenicity of control TIC, challenge with equal numbers of total cultured B16 cells did not produce detectable tumors in WT mice during this period (not shown). As PD-L1 can inhibit tumor rejection through immune mechanisms (21) we next challenged severely immune-deficient NSG mice with TIC from control or PD-L1<sup>lo</sup> B16 TIC. Similar to observations in WT mice, tumor growth was significantly slower (Fig. 2D) and survival significantly longer (Fig. 2E) in NSG mice following PD-L1<sup>lo</sup> versus control B16 TIC challenge. Therefore, PD-L1 control of TIC growth and virulence includes cell autonomous and immune-independent mechanisms.

### TIC PD-L1 promotes TIC self-renewal *in vivo*

To confirm poor self-renewal potential of PD-L1<sup>lo</sup> TIC, we assessed *in vivo* serial TIC passage (20). When tumors generated in NSG mice using TIC as above reached 1800 mm<sup>3</sup>, TIC were sorted from them and transplanted into naïve NSG, producing tumors with kinetics similar to the original transplant (compare Fig. 2F to Fig. 2E). By contrast, serial transplant of PD-L1<sup>lo</sup> B16 TIC from similarly produced original PD-L1<sup>lo</sup> tumors failed to produce tumors in NSG mice even after 150 days, when the experiment was terminated (Fig. 2F). These data corroborate poor *in vitro* self-renewal of PD-L1<sup>lo</sup> B16 TIC, confirm their defective *in vivo* function and demonstrate additional cell autonomous effects.

Total ID8agg control cells formed tumors significantly faster than PD-L1<sup>lo</sup> ID8agg cells in WT mice (median survival 40 days versus 76 days (p<0.0001), respectively, Fig. 2G). Control ID8agg TIC were also significantly more tumorigenic than PD-L1<sup>lo</sup> ID8agg TIC in WT mice (p=0.02, Fig. 2H). These data confirm defective *in vivo* function in B16 and ID8agg PD-L1<sup>lo</sup> TIC.

### PD-L1 promotes TIC genes

To understand mechanisms for PD-L1-mediated TIC effects, we hypothesized that PD-L1 promoted stemness gene expression. We thus assessed the stem cell master transcription factors *nanog*, *sox2* and *pou5f1* (*oct4*) (22). In RNA-seq studies of total cultured ID8agg, these canonical TIC genes produced too few reads for statistics. qPCR analyses of highly purified, sorted B16 and ID8agg TIC demonstrated that *nanog* and *oct4*, but not *sox2* message were significantly higher in control or PD-L1<sup>lo</sup> TIC versus their respective total cultures, and significantly lower in PD-L1<sup>lo</sup> TIC versus respective control TIC (Fig. 3A, B). In further support of PD-L1 control of stemness genes, the ovarian cancer TIC genes *cd24*, *cd117* (*c-Kit*) and *lin28a* (23) and additional TIC genes *nes* and *ck18* were significantly reduced in total ID8agg PD-L1<sup>lo</sup> versus control cells by RNA-seq (Suppl. Table 1). Thus, PD-L1 regulates stemness gene expression, which is a candidate PD-L1-mediated TIC regulation mechanism.

### Cell-intrinsic PD-L1 promotes TIC interferon- $\gamma$ sensitivity

Interferon- $\gamma$  is a potent PD-L1 inducer in tumor cell populations (21). B16 and ID8agg TIC expressed interferon- $\gamma$ -inducible PD-L1, which expression was blunted in PD-L1<sup>lo</sup> TIC as expected (Fig. 4 A, B), and also confirming the stringent PD-L1 knock down effect in clones. We next tested interferon- $\gamma$ -mediated growth suppression. Strikingly, control B16 TIC were more interferon- $\gamma$ -susceptible versus corresponding PD-L1<sup>lo</sup> TIC (Fig. 4C). Further, the absolute numbers of control TIC and non-TIC were similarly reduced by interferon- $\gamma$  treatment (Fig. 4D, E), unlike PD-L1<sup>lo</sup> TIC and non-TIC. Similarly, control ID8agg TIC were more susceptible to interferon- $\gamma$ -mediated growth suppression versus control non-TIC, although it required an ~2.5-fold higher interferon- $\gamma$  concentration to reduce ID8agg versus B16 TIC numbers (Fig. 4F-H). PD-L1<sup>lo</sup> ID8agg non-TIC were more sensitive versus control ID8agg non-TIC to interferon- $\gamma$ -mediated growth suppression, whereas in B16, control and PD-L1<sup>lo</sup> non-TIC were approximately equally sensitive (compare Fig. 4C and 4F). These data suggest that interferon- $\gamma$  signals in TIC can differ from non-TICs, that cell-intrinsic PD-L1 signals can affect interferon- $\gamma$  effects in TIC and



non-TIC, but there are also quantitative as well as qualitative tumor-specific differences that will require much additional work to clarify.

### Cell-intrinsic PD-L1 promotes TIC rapamycin sensitivity

We reported that PD-L1 promotes mTORC1 signals in B16 and ID8agg cells (3). To test functional consequences in TIC, we cultured cells with rapamycin, which preferentially inhibits mTORC1 (24). Growth of control B16 TIC was more rapamycin-sensitive versus corresponding control non-TIC, and in corresponding TIC, control TIC were more sensitive than PD-L1<sup>lo</sup> TIC (Fig. 5A-C). Thus, TIC can also differ in rapamycin-mediated growth suppression versus non-TIC and cell-intrinsic PD-L1 can control this effect in TIC as well as non-TIC. Regulatory associated protein of mTOR (*rptor*) is a positive mTOR regulator that acts as a scaffold for mTORC1 assembly and predicts mTORC1 activity. We used qPCR of highly sort-purified TIC to show that *rptor* expression was significantly reduced in B16 PD-L1<sup>lo</sup> TIC versus respective control TIC (Fig. 5D), consistent with PD-L1-driven mTORC1 signaling in TIC as we reported for total cultures (3), and suggesting reduced mTORC1 dependence as an explanation for reduced rapamycin sensitivity in PD-L1<sup>lo</sup> TIC. Similar to B16, control ID8agg TIC were more sensitive to rapamycin-mediated growth suppression versus PD-L1<sup>lo</sup> TIC, but in contrast to B16, non-TIC were equally sensitive independent of PD-L1 status (compare Fig. 5A-C to Fig. 5E-G). *Rptor* was significantly reduced in ID8agg PD-L1<sup>lo</sup> TIC (Fig. 5H) consistent with PD-L1-driven augmentation of mTORC1 signaling, similar to mTORC1 augmentation in B16 TIC (Fig. 5D).

### Tumor cell intrinsic PD-L1 controls TIC numbers in human ovarian cancer cells

To assess human relevance of our data we studied ES2 human ovarian cancer cells. We previously showed that these are PD-L1<sup>+</sup> and that PD-L1<sup>lo</sup> ES2 cells proliferated more slowly *in vitro* versus control ES2 (3). ALDH1<sup>hi</sup>CD133<sup>+</sup> is an accepted human ovarian cancer TIC phenotype (15, 16). As we found that ES2 cells expressed negligible CD133 by flow cytometry (not shown), we used ALDH<sup>hi</sup> expression to identify ES2 TIC *in vitro*. Control ES2 TIC expressed higher PD-L1 versus control non-TIC (PD-L1 MFI 6300 versus 5437. In contrast to murine cells PD-L1 expression in TIC was not different versus non-TIC PD-L1<sup>lo</sup> clone 1 912 versus 921 and clone 2 1826 versus 1860 for TIC versus non-TIC respectively, Fig. 6A). Further contrasting with mouse cell lines, PD-1 expression by flow cytometry was absent on control and PD-L1<sup>lo</sup> TIC and non-TIC (Fig. 6B). Nonetheless, cell-intrinsic PD-L1 controlled ES2 ovarian cancer TIC numbers *in vitro* (Fig. 6C) as seen in mouse cells (Fig. 1A, B).

### Cell intrinsic PD-L1 controls tumorsphere formation and SOX2 in human ES2 ovarian cancer cells

To assess TIC self-renewal function effects of PD-L1, we found that ES2 TIC cell-specific PD-L1 promoted tumorsphere formation *in vitro* as evidenced by significantly more numerous and bigger spheres than those formed by PD-L1<sup>lo</sup> TIC (Fig. 6C-F). As an alternative for ES2 TIC identification, CD44<sup>+</sup>CD24<sup>-</sup> ES2 cells are also reported to have stem cell properties (16). We sorted CD44<sup>+</sup>CD24<sup>-</sup> ES2 cells and showed that tumorsphere formation was also defective in PD-L1<sup>lo</sup> versus control TIC defined this way (Fig. 6G, H) consistent with the concept that cell-intrinsic PD-L1 in human ES2 cells controls self-

renewal. Further, when we injected ALDH<sup>hi</sup> TIC sorted from ES2 control or PD-L1<sup>lo</sup> cultures into immunodeficient NSG mice, survival was significantly reduced in control versus PD-L1<sup>lo</sup> TIC challenge (Fig. 6I), consistent with reduced TIC tumorigenicity function of PD-L1<sup>lo</sup> ES2 TIC *in vivo*. ES2 TIC overexpress the canonical stem cell genes *SOX2* and *OCT4* (16). We sorted ALDH<sup>hi</sup> ES2 TIC and used qPCR to show that expression of *SOX2* (Fig. 6J, but not *OCT4* or *NANOG* (Suppl. Fig. 4) was significantly reduced in PD-L1<sup>lo</sup> ES2 TIC versus control TIC, but *SOX2* in control or PD-L1<sup>lo</sup> TIC was higher than in respective total cultures. Thus, PD-L1 in human ES2 ovarian cancer cells recapitulates important TIC features and functions seen in the murine cell lines, although PD-L1 influences different stemness genes in these distinct cellular contexts.

### Tumor-intrinsic PD-L1 regulates interferon- $\gamma$ and rapamycin responsiveness in human ES2 ovarian cancer cells

Finally, we investigated the sensitivity of ES2 TIC to growth inhibition by interferon- $\gamma$  and rapamycin. Control ES2 TIC and non-TIC were more sensitive than respective PD-L1<sup>lo</sup> TIC and non-TIC to growth suppression by interferon- $\gamma$  (Fig. 7A-C). PD-L1 similarly rendered ES2 TIC sensitive to rapamycin-mediated growth inhibition. By contrast to ES2 TIC effects, PD-L1 inhibited non-TIC rapamycin-mediated growth inhibition (Fig. 7D-F). mTORC1 signals were reduced comparably to PD-L1<sup>lo</sup> B16 and ID8agg as assessed by *RPTOR* gene expression levels (compare Fig. 7G to Fig. 5D, H).

## Discussion

Mechanisms regulating TIC generation, proliferation and virulence remain incompletely understood. Since the initial observation that tumor cell-expressed PD-L1 (B7-H1) can kill T cells (1), the focus of PD-L1 effects on tumor immunopathology has been on cell-extrinsic inhibitory signals to PD-1<sup>+</sup> T cells (1, 2, 17, 25). We recently reported that tumor PD-L1 regulates cell-autonomous immune-independent tumor growth, mTOR and autophagy in melanoma and ovarian cancer cells (3). In this study, we show additional significant, previously unrecognized effects of tumor intrinsic PD-L1 on TIC generation, proliferation, canonical TIC gene expression and treatment responses differing from known tumor extrinsic PD-L1 effects, and demonstrate their human relevance.

PD-L1 is expressed by cancer stem cells in human glioma (7), squamous cell carcinoma of the head and neck (9) and colon cancer where PD-L1 was higher than non-stem cells (8), but a mechanistic relationship between PD-L1 and stem cell generation or function was not defined. We show here that TIC express higher PD-L1 levels than non-TIC in mouse melanoma and mouse but not in human ovarian cancer. This cell-intrinsic PD-L1 controlled numbers of TIC generated *in vitro* in mouse B16 melanoma and ID8agg ovarian cancer and in human ES2 ovarian cancer cells. Thus, this novel capacity of cell-intrinsic PD-L1 to promote TIC is not confined to a single tumor type and is also relevant to human cancer. The significance of higher PD-L1 expression in some TIC versus non-TIC is uncertain, but could relate to additional TIC-specific signaling in differing tumor cell types. In human head and neck cancers, cancer stem cells defined solely by CD44 expression and sorted into PD-L1<sup>+</sup> and PD-L1<sup>-</sup> populations effected comparable tumorigenicity in NSG mice, whereas PD-L1<sup>+</sup>



stem cells elicited more evidence for T cell dysfunction *in vitro* versus PD-L1<sup>-</sup> stem cells (9). By contrast, we show here that PD-L1<sup>lo</sup> TICs in melanoma and ovarian cancer had poor tumorigenicity in immune sufficient and immune deficient mice, thus confirming that TIC-intrinsic PD-L1 has unexpected TIC growth promoting effects in melanoma and ovarian cancer cells, in addition to anticipated immune evasive effects. PD-L1 mediates an immune evasive role in all cancers and TIC tested thus far. The lack of clear PD-L1-mediated immune-independent TIC growth promotion in head and neck cancers that contrasts with our data in melanoma and ovarian cancer cells suggests that cell-intrinsic PD-L1 growth promotion also depends on tumor-specific properties yet to be defined, an area worthy of additional study. This head and neck study also tested few mice and did not assess different TIC challenge numbers that could help explain divergent outcomes.

We recently showed that in total B16 and ID8agg cell cultures, tumor PD-L1 promoted tumor cell proliferation and mTORC1 activation (3). We show here that PD-L1 increased the mTORC1 component *rptor* in B16 and ID8agg TIC, and also in human ES2 TIC, consistent with increased mTORC1 signals. The preferential mTORC1 inhibitor rapamycin reduced control (PD-L1-replete) B16, ID8agg TIC numbers *in vitro* with significantly diminished effects on PD-L1<sup>lo</sup> TIC, consistent with the concept that PD-L1-driven mTORC1 promotes TIC generation in these cells. TIC PD-L1 also sensitized human ES2. TIC are considered to be treatment resistant, but we show that TIC PD-L1 sensitizes TIC to the small molecule mTORC1 inhibitor rapamycin. This observation deserves additional exploration, including assessing other mTORC1 or dual mTORC1/2 inhibitors. Our data predict that efficacy of  $\alpha$ PD-L1 in PD-L1<sup>+</sup> tumors for which  $\alpha$ PD-L1 is most likely to be effective (26, 27) could be enhanced in some cases when combined with an appropriate mTOR inhibitor.

Interferon- $\gamma$ -induced PD-L1 regulation is well-known (27). Thus, as expected, interferon- $\gamma$  augmented TIC PD-L1 expression. However, we show here that PD-L1 also appears to alter interferon- $\gamma$  signals, as TIC PD-L1 unexpectedly sensitized murine B16 and ID8agg TIC, and human ES2 TIC, to interferon- $\gamma$ -mediated growth suppression *in vitro*. These data demonstrate the first TIC immune sensitizing mechanism to our knowledge. In adaptive immune resistance, the incoming immune response, including interferon- $\gamma$ , makes the tumor resist further immune attack (28). TIC PD-L1 might suppress anti-tumor T cell responses as seen in studies of total tumors (1, 21) and head and neck cancer TIC (9), yet TIC PD-L1 could render them more vulnerable to immune mediated clearance. This complexity requires much additional study to understand in which TIC their PD-L1 alters immune effects on tumor and to optimize immunotherapy treatment strategies. For example, our work suggests that  $\alpha$ PD-L1 plus interferon- $\gamma$ , T cells producing interferon- $\gamma$  (such as TIC-targeting CAR T cells) or perhaps interferon- $\alpha$  are strategies for further testing in TIC in which PD-L1 sensitizes them to interferon- $\gamma$ -mediated growth inhibition.

In assessing mechanisms for TIC generation, we found that PD-L1 signals promoted canonical stemness gene expression. In mouse B16 melanoma and ID8agg ovarian cancer cells, PD-L1 augmented expression of *oct4* and *nanog*, but not *sox2*. By contrast, PD-L1 promoted *SOX2* but not *OCT4* or *NANOG* in human ES2 ovarian cancer cells. These data are consistent with the notion that PD-L1-driven stemness gene expression is a mechanism for its capacity to generate TIC. Our data further suggest that the specific stemness genes

driving TIC depend on the tumor, likely reflecting differing mutational landscapes in ovarian cancers versus melanomas (29, 30), and also helping understand the many cell-specific outcomes we define here in regards also to rapamycin and interferon- $\gamma$  sensitivity. Mechanisms for how PD-L1 alters gene expression requires further study. Effects are transcriptional as evidenced by reduced canonical stem cell gene message in PD-L1<sup>lo</sup> TIC we show here and in our recent work on non-TIC (3), but how PD-L1 effects transcriptional control remains to be defined. Regulation could also be through mTOR-related translational effects (31). Understanding these specific mechanisms could define novel means to reduce TIC generation.

PD-1, a major PD-L1 receptor, was recently shown to regulate cell-intrinsic and immune-independent melanoma growth in mouse and human melanoma cells (10). B7-H3, like PD-1 and PD-L1 is an immunoglobulin superfamily member. These three molecules all exert tumor cell-intrinsic effects, including regulating tumor mTOR, its regulators or its targets (3, 10, 32). As mTOR could play a critical role in TIC generation (33), the concept that tumor cell-intrinsic immunoglobulin superfamily members exert related, important signaling effects in cancer immunopathogenesis or treatment responses merits much additional attention.

In summary, we show that tumor PD-L1 effects are considerably broader than simply blunting PD-1<sup>+</sup> anti-tumor T cell activities and suggest many additional avenues for investigations of tumor immunopathogenesis, treatment approaches and potentially treatment responses. Given the virulence and treatment resistance of TIC, such studies could also help develop successful new treatment approaches that specifically target TIC. Finally, immune checkpoint molecules in the immunoglobulin superfamily could have common tumor cell-intrinsic properties that will expand our understanding of their contributions to cancer pathogenesis and provide insights into effective cancer treatments.

## Supplementary Material

Refer to Web version on PubMed Central for supplementary material.

## Acknowledgments

Thanks to Andrew Brenner for help in establishing tumorsphere cultures.

Financial support: Tyler Curiel (CA170491, CA054174, CDMRP, The Holly Beach Public Library, The Owens Foundation, The Ovarian Cancer Research Fund Alliance, The Barker Foundation and the Skinner endowment).

## Literature cited

1. Dong H, Strome SE, Salomao DR, Tamura H, Hirano F, Flies DB, et al. Tumor-associated B7-H1 promotes T-cell apoptosis: A potential mechanism of immune evasion. *Nat Med.* 2002; 8:793–800. [PubMed: 12091876]
2. Brahmer JR, Tykodi SS, Chow LQ, Hwu WJ, Topalian SL, Hwu P, et al. Safety and activity of anti-PD-L1 antibody in patients with advanced cancer. *N Engl J Med.* 2012; 366:2455–65. [PubMed: 22658128]
3. Clark CA, Gupta H, Sareddy GR, Pandeswara S, Lao S, Yuan B, et al. Tumor-intrinsic PD-L1 signals regulate cell growth, pathogenesis and autophagy in ovarian cancer and melanoma. *Cancer Res.* 2016; in press. doi: 10.1158/0008-5472.CAN-16-0258

4. Chang CH, Qiu J, O'Sullivan D, Buck MD, Noguchi T, Curtis JD, et al. Metabolic Competition in the Tumor Microenvironment Is a Driver of Cancer Progression. *Cell*. 2015; 162:1229–41. [PubMed: 26321679]
5. Boiko AD, Razorenova OV, van de Rijn M, Swetter SM, Johnson DL, Ly DP, et al. Human melanoma-initiating cells express neural crest nerve growth factor receptor CD271. *Nature*. 2010; 466:133–7. [PubMed: 20596026]
6. Li Y, Rogoff HA, Keates S, Gao Y, Murikipudi S, Mikule K, et al. Suppression of cancer relapse and metastasis by inhibiting cancer stemness. *Proc Natl Acad Sci U S A*. 2015; 112:1839–44. [PubMed: 25605917]
7. Yao Y, Tao R, Wang X, Wang Y, Mao Y, Zhou LF. B7-H1 is correlated with malignancy-grade gliomas but is not expressed exclusively on tumor stem-like cells. *Neuro Oncol*. 2009; 11:757–66. [PubMed: 19264916]
8. Zhi Y, Mou Z, Chen J, He Y, Dong H, Fu X, et al. B7H1 Expression and Epithelial-To-Mesenchymal Transition Phenotypes on Colorectal Cancer Stem-Like Cells. *PLoS One*. 2015; 10:e0135528. [PubMed: 26284927]
9. Lee Y, Shin JH, Longmire M, Wang H, Kohrt HE, Chang HY, et al. CD44+ Cells in Head and Neck Squamous Cell Carcinoma Suppress T-Cell-Mediated Immunity by Selective Constitutive and Inducible Expression of PD-L1. *Clin Cancer Res*. 2016; 22:3571–81. [PubMed: 26864211]
10. Kleffel S, Posch C, Barthel SR, Mueller H, Schlapbach C, Guenova E, et al. Melanoma Cell-Intrinsic PD-1 Receptor Functions Promote Tumor Growth. *Cell*. 2015; 162:1242–56. [PubMed: 26359984]
11. Roby KF, Taylor CC, Sweetwood JP, Cheng Y, Pace JL, Tawfik O, et al. Development of a syngeneic mouse model for events related to ovarian cancer. *Carcinogenesis*. 2000; 21:585–91. [PubMed: 10753190]
12. Curiel TJ, Wei S, Dong H, Alvarez X, Cheng P, Mottram P, et al. Blockade of B7-H1 improves myeloid dendritic cell-mediated antitumor immunity. *Nat Med*. 2003; 9:562–7. [PubMed: 12704383]
13. Dou J, Pan M, Wen P, Li Y, Tang Q, Chu L, et al. Isolation and identification of cancer stem-like cells from murine melanoma cell lines. *Cell Mol Immunol*. 2007; 4:467–72. [PubMed: 18163959]
14. Gil M, Komorowski MP, Seshadri M, Rokita H, McGray AJ, Opyrchal M, et al. CXCL12/CXCR4 blockade by oncolytic virotherapy inhibits ovarian cancer growth by decreasing immunosuppression and targeting cancer-initiating cells. *J Immunol*. 2014; 193:5327–37. [PubMed: 25320277]
15. Kryczek I, Liu S, Roh M, Vatan L, Szeliga W, Wei S, et al. Expression of aldehyde dehydrogenase and CD133 defines ovarian cancer stem cells. *Int J Cancer*. 2012; 130:29–39. [PubMed: 21480217]
16. Liang D, Ma Y, Liu J, Trope CG, Holm R, Nesland JM, et al. The hypoxic microenvironment upgrades stem-like properties of ovarian cancer cells. *BMC Cancer*. 2012; 12:201. [PubMed: 22642602]
17. Lin PY, Sun L, Thibodeaux SR, Ludwig SM, Vadlamudi RK, Hurez VJ, et al. B7-H1-Dependent Sex-Related Differences in Tumor Immunity and Immunotherapy Responses. *J Immunol*. 2010; 185:2747–53. [PubMed: 20686128]
18. Facciabene A, Peng X, Hagemann IS, Balint K, Barchetti A, Wang LP, et al. Tumour hypoxia promotes tolerance and angiogenesis via CCL28 and T(reg) cells. *Nature*. 2011; 475:226–30. [PubMed: 21753853]
19. Schatton T, Schutte U, Frank NY, Zhan Q, Hoerning A, Robles SC, et al. Modulation of T-cell activation by malignant melanoma initiating cells. *Cancer Res*. 2010; 70:697–708. [PubMed: 20068175]
20. Civenni G, Walter A, Kobert N, Mihic-Probst D, Zipser M, Belloni B, et al. Human CD271-positive melanoma stem cells associated with metastasis establish tumor heterogeneity and long-term growth. *Cancer Res*. 2011; 71:3098–109. [PubMed: 21393506]
21. Spranger S, Spaepen RM, Zha Y, Williams J, Meng Y, Ha TT, et al. Up-regulation of PD-L1, IDO, and T(regs) in the melanoma tumor microenvironment is driven by CD8(+) T cells. *Sci Transl Med*. 2013; 5:200ra116.

22. Radzisheuskaya A, Silva JC. Do all roads lead to Oct4? the emerging concepts of induced pluripotency. *Trends Cell Biol.* 2014; 24:275–84. [PubMed: 24370212]
23. Peng S, Maihle NJ, Huang Y. Pluripotency factors Lin28 and Oct4 identify a sub-population of stem cell-like cells in ovarian cancer. *Oncogene.* 2010; 29:2153–9. [PubMed: 20101213]
24. Hurez V, Dao V, Liu A, Pandeswara S, Gelfond J, Sun L, et al. Chronic mTOR inhibition in mice with rapamycin alters T, B, myeloid, and innate lymphoid cells and gut flora and prolongs life of immune-deficient mice. *Aging Cell.* 2015; 14:945–56. [PubMed: 26315673]
25. Topalian SL, Drake CG, Pardoll DM. Targeting the PD-1/B7-H1(PD-L1) pathway to activate anti-tumor immunity. *Curr Opin Immunol.* 2012; 24:207–12. [PubMed: 22236695]
26. Pardoll DM. The blockade of immune checkpoints in cancer immunotherapy. *Nat Rev Cancer.* 2012; 12:252–64. [PubMed: 22437870]
27. Topalian SL, Taube JM, Anders RA, Pardoll DM. Mechanism-driven biomarkers to guide immune checkpoint blockade in cancer therapy. *Nat Rev Cancer.* 2016; 16:275–87. [PubMed: 27079802]
28. Taube JM, Anders RA, Young GD, Xu H, Sharma R, McMiller TL, et al. Colocalization of inflammatory response with B7-h1 expression in human melanocytic lesions supports an adaptive resistance mechanism of immune escape. *Sci Transl Med.* 2012; 4:127ra37.
29. Hodis E, Watson IR, Kryukov GV, Arold ST, Imielinski M, Theurillat JP, et al. A landscape of driver mutations in melanoma. *Cell.* 2012; 150:251–63. [PubMed: 22817889]
30. Integrated genomic analyses of ovarian carcinoma. *Nature.* 2011; 474:609–15. [PubMed: 21720365]
31. Hsieh AC, Liu Y, Edlind MP, Ingolia NT, Janes MR, Sher A, et al. The translational landscape of mTOR signalling steers cancer initiation and metastasis. *Nature.* 2012
32. Jiang B, Liu F, Liu Z, Zhang T, Hua D. B7-H3 increases thymidylate synthase expression via the PI3k-Akt pathway. *Tumour Biol.* 2016; 37:9465–72. [PubMed: 26787540]
33. Ghosh J, Kobayashi M, Ramdas B, Chatterjee A, Ma P, Mali RS, et al. S6K1 regulates hematopoietic stem cell self-renewal and leukemia maintenance. *J Clin Invest.* 2016; 126:2621–5. [PubMed: 27294524]

### Significance

Studies of PD-L1 signals in tumor immunopathogenesis and treatment responses have focused on cell-extrinsic effects. We introduce a major shift from the current paradigm by showing novel cell-intrinsic PD-L1 signaling that promotes TIC generation, virulence, and treatment responses, greatly augmenting understanding of PD-L1 signals in cancer pathogenesis and treatment responses.

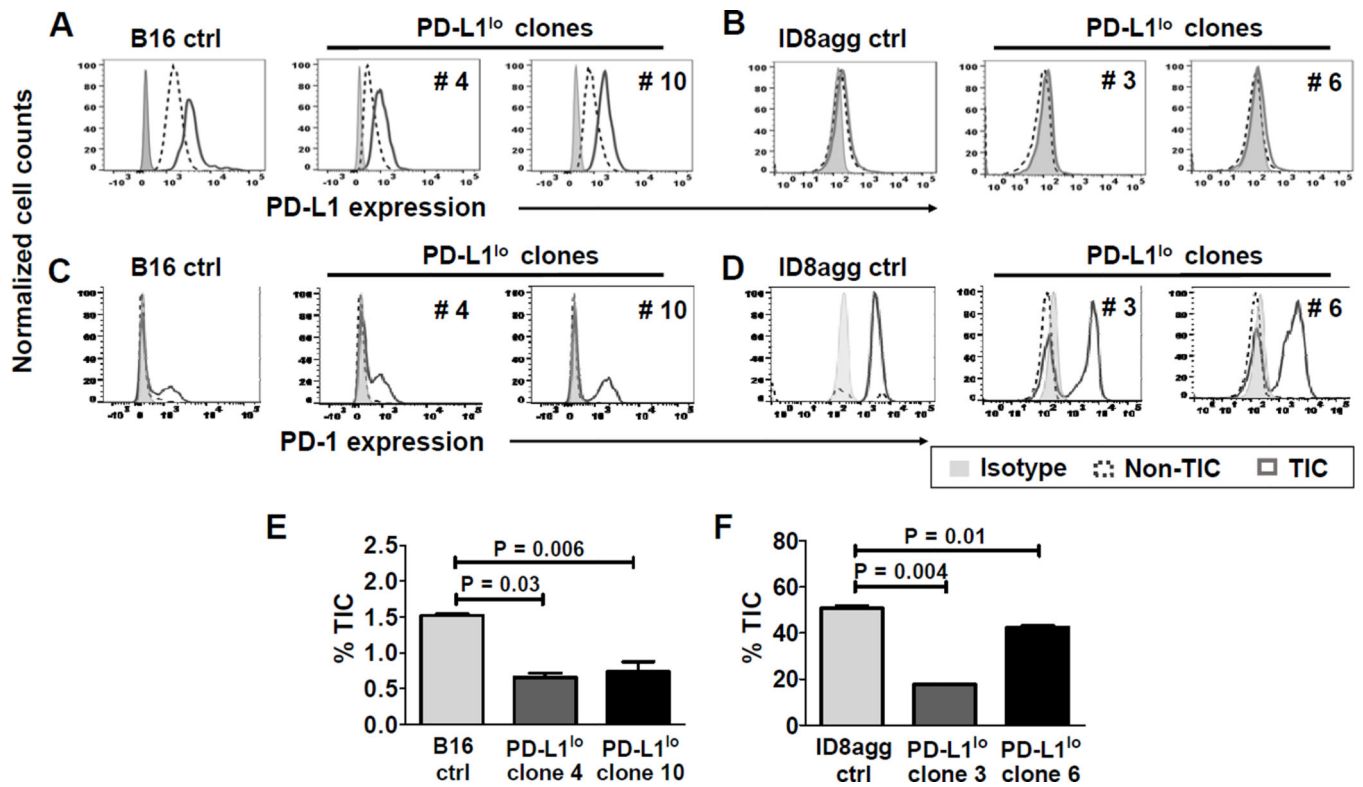


**Figure 1. PD-L1 expression is higher on TIC versus non-TIC and regulates TIC numbers *in vitro*** PD-L1 expression by flow cytometry in cultures of B16 (A) and ID8agg cells (B). PD-1 expression by flow cytometry in cultures of B16 (C) and ID8agg (D). TIC percentage for B16 (CD44<sup>+</sup>CD133<sup>+</sup>CD24<sup>+</sup> cells, E), ID8agg (CD44<sup>+</sup>CD24<sup>+</sup> cells, F) and respective PD-L1<sup>lo</sup> clones by flow cytometry of cultured cells. P values, unpaired *t* test. Ctrl, control.



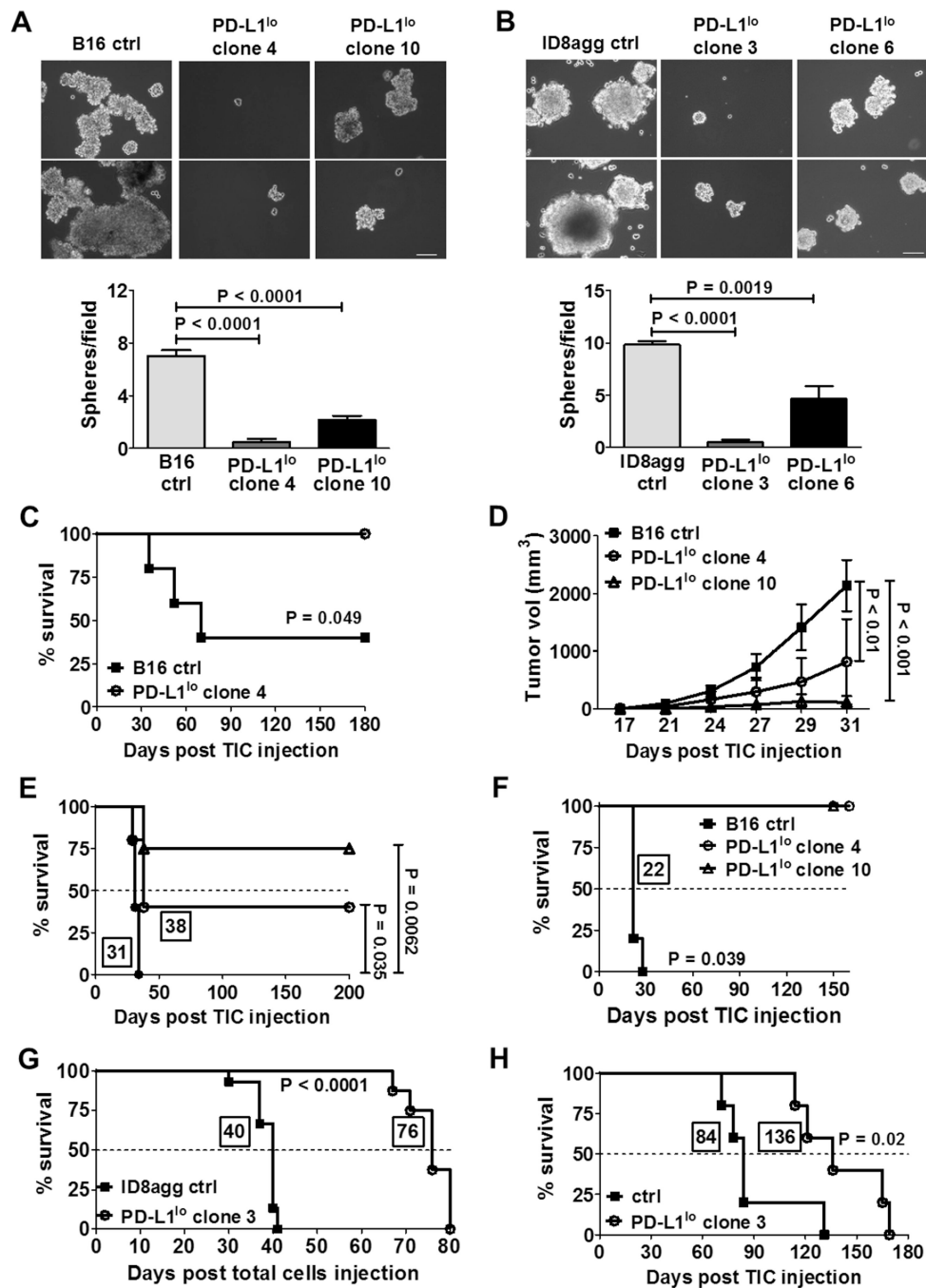


### Figure 2. PD-L1<sup>lo</sup> B16 and ID8agg TIC are functionally defective

Representative photomicrographs of tumorspheres after 14 days in culture of B16 (A) or ID8agg (B) control (ctrl) and PD-L1<sup>lo</sup> clones. Bars equal 100  $\mu$ M. Summary data below. At least 6 fields assessed/clone. P values, unpaired *t* test. (C) Survival of WT mice injected with 5000 indicated, sorted TIC (n=5–6/group). P value, log-rank test. (D) Tumor growth in NSG mice injected with indicated, sorted 10<sup>4</sup> B16 TIC (n=5/group). P value, two-way ANOVA. (E) Survival of mice in (D). (F) Tumor growth in NSG mice injected with TIC sorted from tumors in (D). P value, log rank test for trend. (G) Survival of WT mice injected i.p. with 4

$\times 10^6$  total indicated ID8agg cells. **(H)** Survival of WT mice injected with  $0.15 \times 10^6$  ID8agg ctrl or PD-L1<sup>lo</sup> clone 3 TIC. P value, log rank test. In panels **E-H**, boxed numbers indicate median survival (days).

Author Manuscript

Author Manuscript

Author Manuscript

Author Manuscript

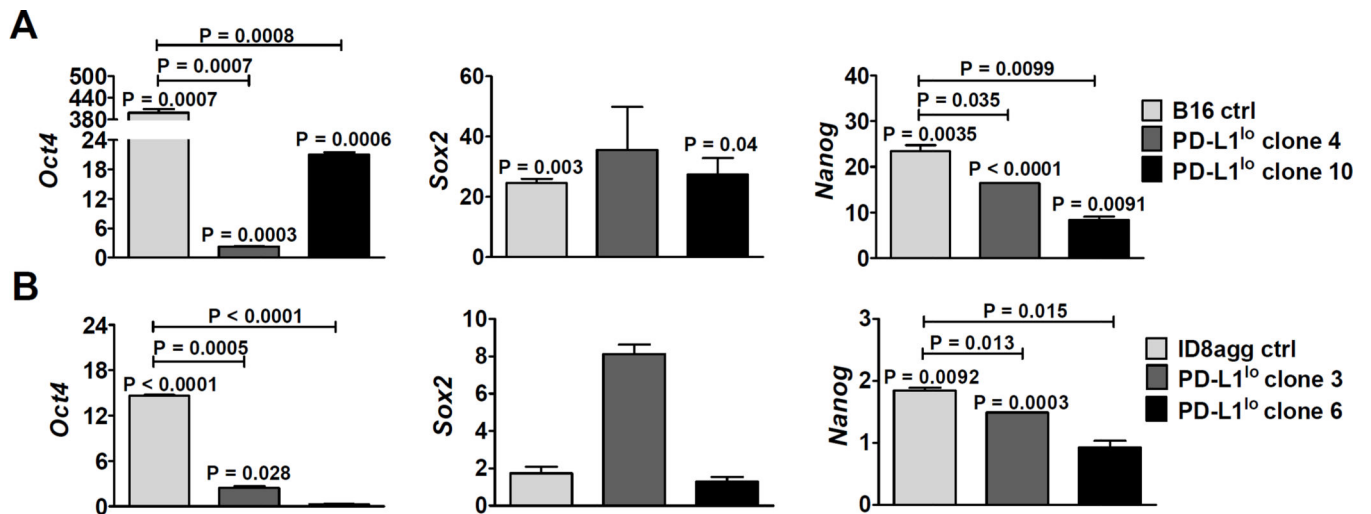


**Figure 3.**

Fold change in gene expression (qPCR) of *Oct4*, *Sox2* and *Nanog* in B16 (A) and ID8agg (B) cells. P values, unpaired *t* test. Each bar represents fold increase in stemness gene expression in TIC versus respective total cultures, with P value for same directly over bar. P values on horizontal lines compare fold changes between ctrl and PD-L1<sup>lo</sup> cultures. Ctrl, control.

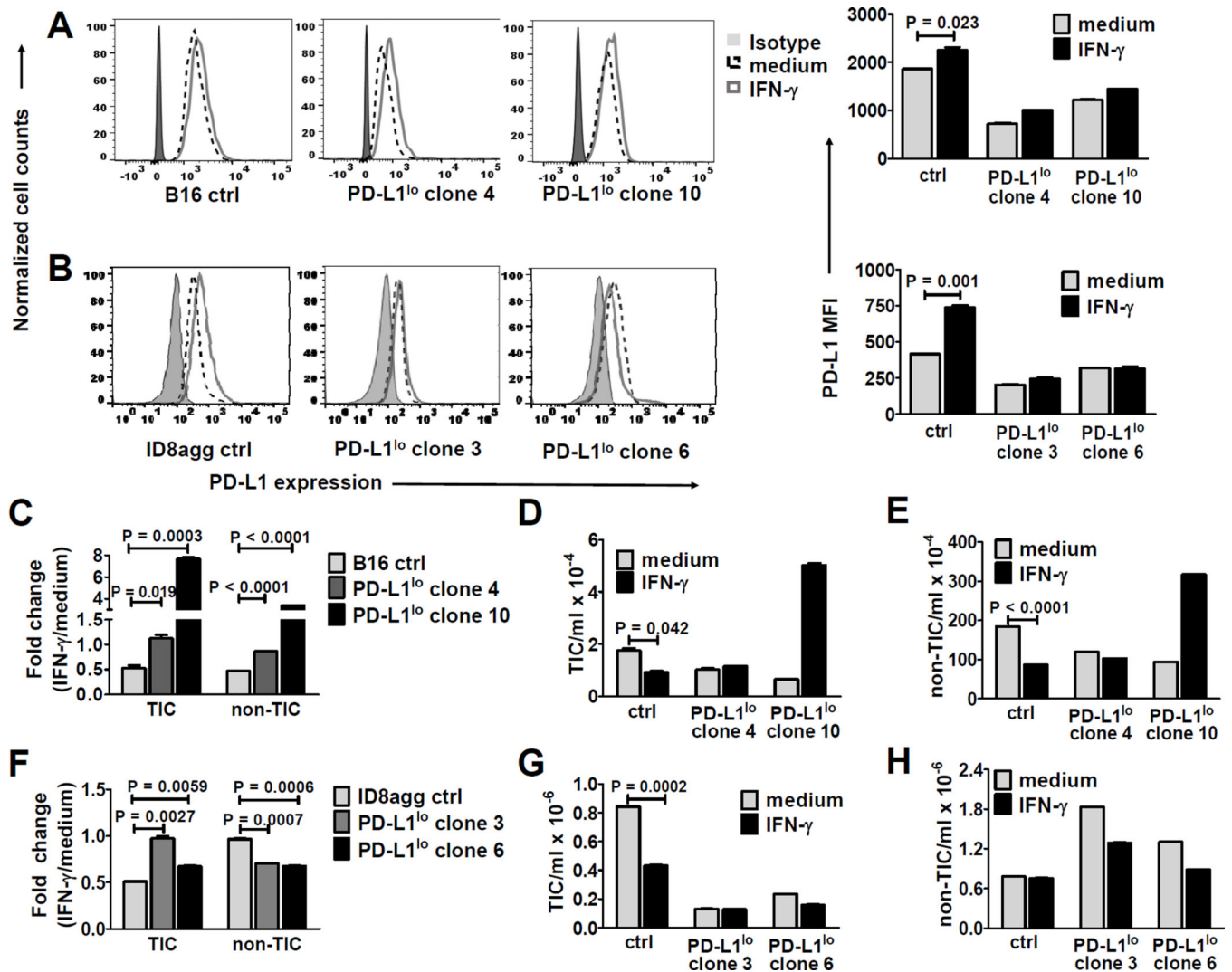


**Figure 4. PD-L1 sensitizes B16 and ID8agg TIC to interferon- $\gamma$**

Representative flow cytometry data for TIC PD-L1 expression on B16 (A) and ID8agg (B) cells treated with 0.2 ng/ml IFN- $\gamma$  for 48 hours, with summary PD-L1 mean fluorescence intensity (MFI) on the right. P values, unpaired *t* test. Absolute cell numbers for B16 (A) or ID8agg (B) TIC or non-TIC after 0.2 ng/ml (B16) or 0.5 ng/ml (ID8agg) interferon- $\gamma$  for 48 hours, versus medium alone. Fold change in B16 (C) TIC or non-TIC numbers after 0.2 ng/ml for 48 hours, versus medium alone. Absolute numbers of B16 TIC (D) and non-TIC (E). Fold change in ID8agg (F) TIC and non-TIC treated with 0.5 ng/ml interferon- $\gamma$  for 48 hours, versus medium alone. P values, unpaired *t* test. Absolute numbers of ID8agg TIC (G) and non-TIC (H). Ctrl, control. IFN-interferon- $\gamma$ .

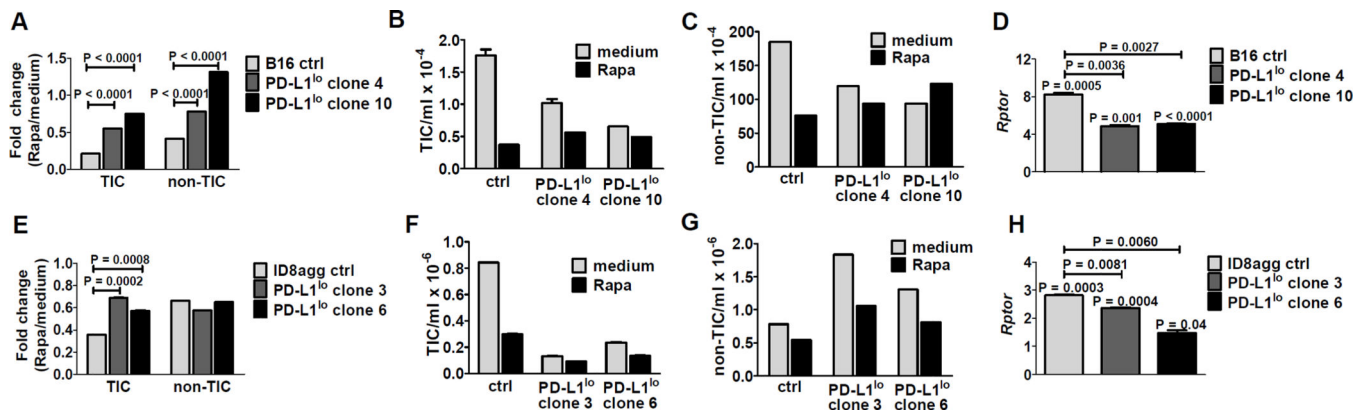


**Figure 5. TIC PD-L1 sensitizes B16 and ID8agg to rapamycin**

Fold change in numbers of B16 (A) TIC and non-TIC treated with 1.5 nM rapamycin for 48 hours, versus medium alone. P values, unpaired *t* test. Absolute numbers of B16 TIC (B) and non-TIC (C). (D) Fold change in B16 *Rptor* expression by qPCR. Each bar represents fold increase in gene expression in TIC versus respective total cultures, with P value for same directly over bar. P values on horizontal lines compare fold changes between control (ctrl) and PD-L1<sup>lo</sup> cultures. Fold change in numbers of ID8agg (E) TIC and non-TIC treated similarly with 1.5 nM rapamycin for 48 hours, versus medium alone. Absolute numbers of ID8agg TIC (F) and non-TIC (G). (H) ID8agg *Rptor* expression by qPCR. P values, unpaired *t* test.

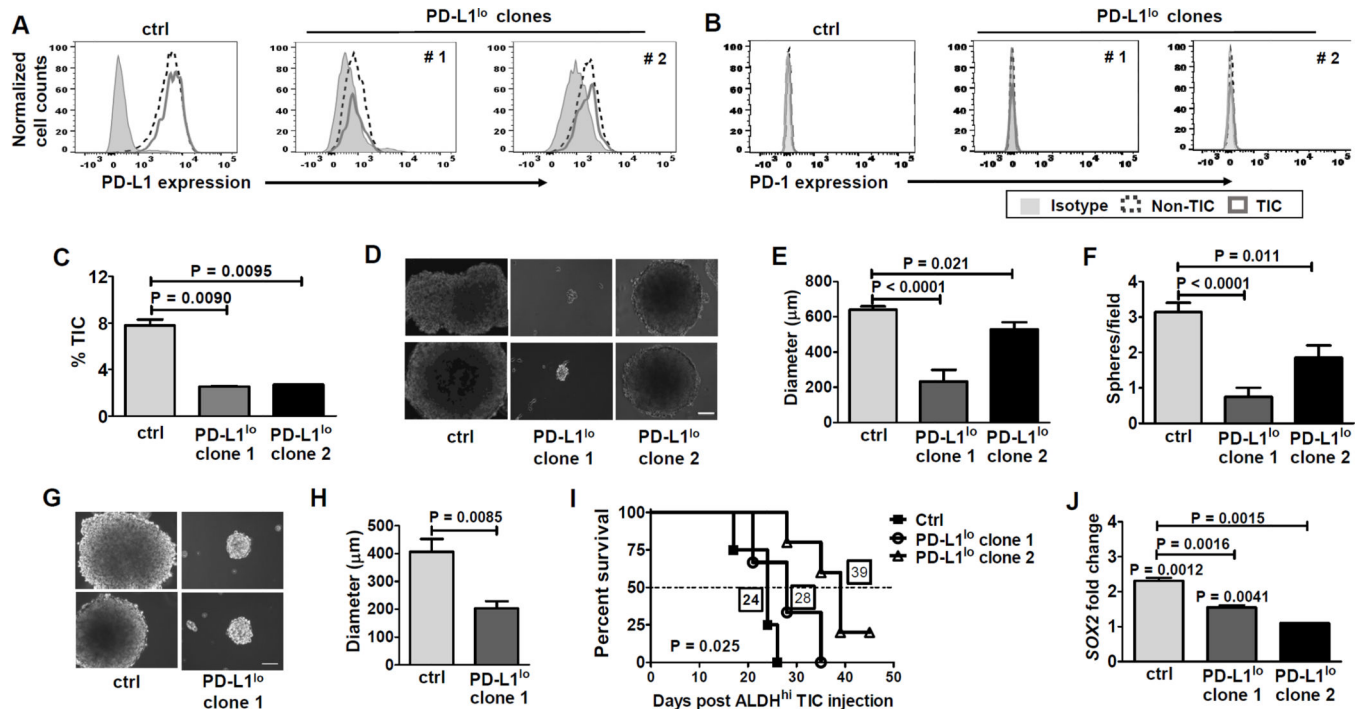


**Figure 6. Human ES2 ovarian cancer cell TIC express PD-L1 that regulates self-renewal, immune-independent tumorigenicity and *SOX2***

PD-L1 (A) or PD-1 (B) expression in control (ctrl) and PD-L1<sup>lo</sup> ES2 TIC by flow cytometry.

(C) Percent of ALDH<sup>hi</sup> TIC by flow cytometry of cultured cells. P values, unpaired *t* test.

(D) Representative photomicrographs of ES2 tumorospheres. Bar equals 100 μM.

Quantification of the size (E) and number of spheres/field (F). P values, unpaired *t* test. (G)

Representative photomicrographs of tumorospheres formed by CD44<sup>+</sup>CD24<sup>-</sup> TIC from control or PD-L1<sup>lo</sup> clone 1 after 14 days, and their diameter (H). (I) Survival curve of NSG mice injected with 20,000 ALDH<sup>hi</sup> TIC indicated (n=3–5/group). Median survival (days) in boxes by individual curves. P value, log-rank test. (J) *SOX2* expression by qPCR from ALDH<sup>hi</sup> TIC and total cultures. Fold changes by CT between TIC and respective total cultures. These fold changes were compared between control and PD-L1<sup>lo</sup> clones. All P values calculated, unpaired *t* test.



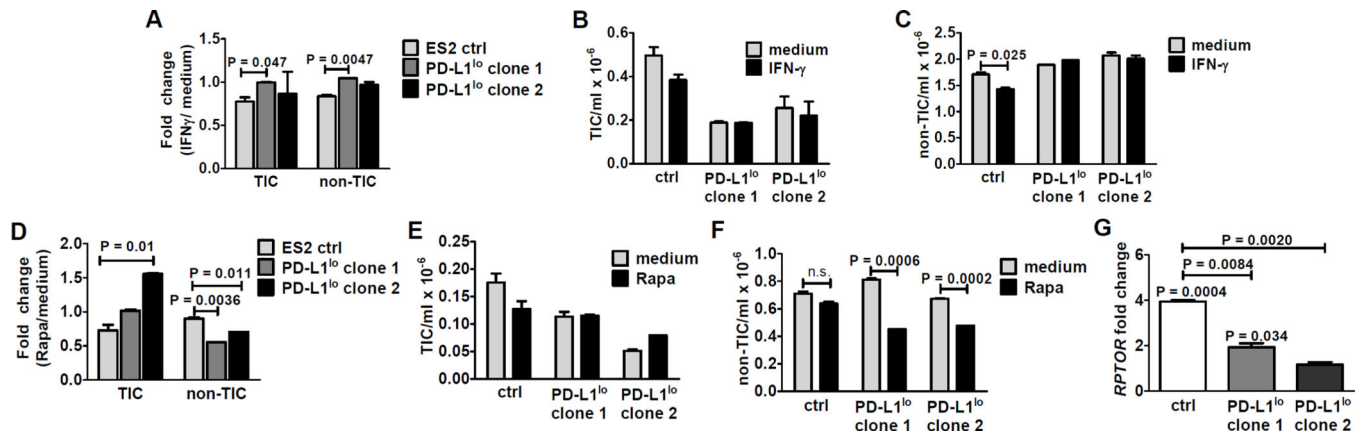


**Figure 7. Human ES2 ovarian cancer TIC PD-L1 alters rapamycin (rapa) and interferon (IFN)- $\gamma$  sensitivity**

(A) Fold change in numbers of ES2 TIC and non-TIC treated with 0.5 ng/ml interferon- $\gamma$  for 60 hours, versus medium alone. P values, unpaired *t* test. Absolute numbers of TIC (B) and non-TIC (C). Fold change in numbers of ES2 TIC (D) and non-TIC treated similarly with 5 nM rapamycin for 60 hours, versus medium alone. Absolute numbers of TIC (E) and non-TIC (F). (G) Fold change in *RPTOR* expression by qPCR. Each bar represents fold increase in gene expression in TIC versus respective total cultures, with P value for same directly over bar. P values on horizontal lines compare fold changes between ctrl and PD-L1<sup>lo</sup> cultures. All P values, unpaired *t* test.